Synthesis and characterization of dendrimer-templated mesoporous oxidation catalysts

Matt C. Rogers, Bamidele Adisa, and David A. Bruce*

Department of Chemical Engineering, Clemson University, Clemson, SC 29634-0909

Received 11 March 2004; accepted 6 August 2004

We report here the use of 4th and 5th generation dendrimers poly(propylene)imine (CU-D32 and CU-D64) as templating agents for the synthesis of mesoporous titanosilicate and vanadosilicate oxidation catalysts via sol–gel techniques. The physical properties of these mesoporous materials were characterized by TGA, BET, PXD and SEM/EDX analyses and these showed that the transition metals are evenly distributed throughout these silicates, which have interconnected spherical pores (approx. 12 Å in diameter) and high surface areas of about 650 $m^2 g^{-1}$. Kinetic studies showed that all transition metal-doped catalysts were highly selective at oxidizing cyclohexene to the corresponding epoxide. Additionally, CU-D64-templated catalysts were more catalytically active for cyclohexene epoxidation than CU-D32-templated catalysts as a result of differences in pore size. All CU-D64-templated catalysts exhibited epoxidation catalytic activity comparable to that of titanium doped MCM-41 materials.

KEY WORDS: dendrimer, mesoporous, oxidation catalyst, sol–gel, vanadosilicate, titanosilicate, cyclohexene, epoxidation.

1. Introduction

The selective oxidation of an olefinic bond is an essential step in the production of numerous fine chemicals and pharmaceuticals [1–6]. In recent years, several heterogeneous and homogeneous catalysts have been shown to be effective in the selective oxidation of alkenes [7–11]. Of the heterogeneous catalysts studied, mesoporous oxide materials have in many cases proven to be ideal because of their high surface areas, large pore diameters, mechanical strength, and controllable surface properties [12–13]. One of the most widely studied groups of mesoporous oxidation catalysts are derived from the silica-based family of highly ordered mesoporous materials known as M41S [14]. These materials, such as MCM-41, are prepared via sol–gel methods using surfactant structure-directing agents [14]. The catalytically active forms of these mesoporous oxides are readily synthesized via the impregnation of transition metals to yield metal-supported catalysts with high metal dispersions [15–21]. For example, researchers have shown that MCM-41 can be impregnated with small amounts of Ti (~2 wt%) to produce an effective catalyst for the selective oxidation of alkenes under mild conditions [20–22].

It is well known that structural changes in a catalyst can lead to significant changes in product selectivity [23–27]. Since the final structure of sol–gel-based materials is dependent upon the structure of the template that was used to create it [14], a change in the templating agent can lead to significant changes in the physical structure and therefore, the chemical nature of the catalyst. In order to better manipulate the pore size and shape of mesoporous materials, Larsen and co-workers [28–31] have recently substituted a variety of amine-terminated dendrimers for the surfactant templates that are commonly used to synthesize mesoporous oxide materials. The result of this substitution was the creation of new mesoporous materials with high surface areas and interconnected spherical shaped pores.

Currently, only two types of amine-terminated dendrimers have been used to synthesize mesoporous silicate materials. The first dendrimer template studied was a Starburst polyamidoamine (PAMAM) dendrimer [28,32]. While the PAMAM dendrimer (4th generation) was an effective template for the synthesis of a mesoporous oxide, the resulting material had poor structural properties that led to pore collapse at elevated temperatures; hence, it proved ineffective for use as a catalyst or support material [29]. In an effort to overcome these shortcomings, poly(propylene)imine (DAB-Am) dendrimer templates were examined by Larsen and co-workers [29–30]. These amine terminated DAB-Am dendrimers (4th and 5th generation) proved to be more effective at templating the synthesis of structurally stable mesoporous silicates with interconnected spherical pores. Larsen and Velarde-Ortiz [31] then extended this work by adding transition metals (e.g., copper) to the sol–gel mixture so that the resulting mesoporous silicates could be more easily characterized; however, no catalytic testing was reported for these doped materials.

In this work, we further investigate the use of two commercially available polypropyleneimine dendrimers

---

* To whom correspondence should be addressed.
E-mail: dbruce@clemson.edu

1011-372X/04/1000–0036/0 © 2004 Plenum Publishing Corporation

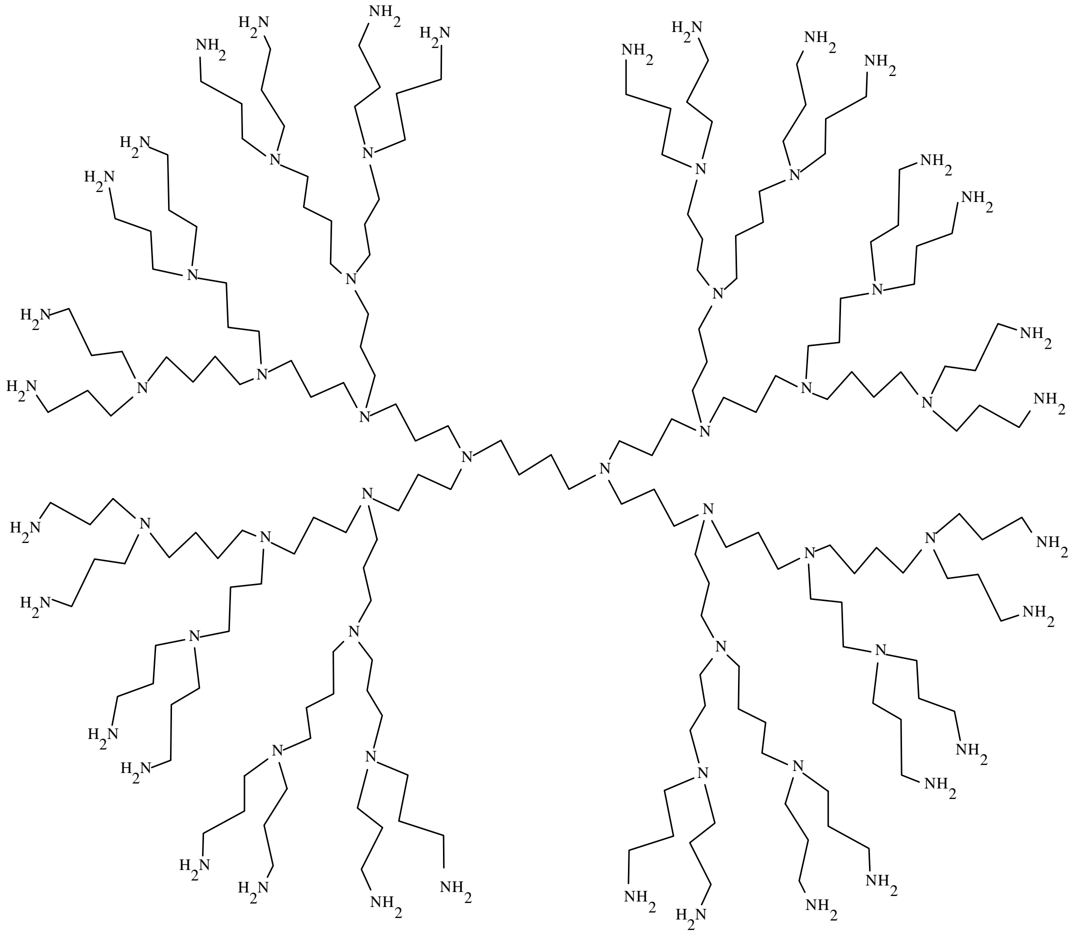

Figure 1. Polypropyleneimine trihexacontaamine, 4th generation polypropyleneimine dendrimer with 32 amine terminating groups (CU-D32).

as structure-directing agents in the production of mesoporous, selective oxidation catalysts. Both the 4th generation DAB-Am dendrimer, polypropyleneimine trihexacontaamine (CU-D32, see figure 1) and the 5th generation DAB-Am dendrimer, polypropyleneimine tetrahexacontaamine (CU-D64) were used to produce a total of eight types of mesoporous oxide catalysts containing either low or high loadings of titanium or vanadium. An additional two samples were prepared using CU-D32 and CU-D64 templates without incorporating any transition metal into the materials. Finally, titanium-doped (MCM-41-Ti) and vanadium-doped (MCM-41-V) MCM-41 materials were prepared in order to compare the performance of the dendrimer-templated materials with that of the more widely studied surfactant-templated MCM materials.

The physical and chemical properties of each of the twelve materials were ascertained using a variety of experimental techniques. Surface area and pore volume were determined for all materials, and scanning electron micrographs (SEM) were collected on selected samples. Temperature-programed pyrolysis and oxidation analysis was performed on selected samples to determine the temperature stability of the precalcined materials. Finally, selective oxidation kinetic studies were performed in a continuously stirred batch reactor using *t*-butyl hydroperoxide as the oxidant and cyclohexene as a test reagent.

2. Experimental

2.1. Preparation of mesoporous catalyst materials

Novel mesoporous oxidation catalysts were synthesized via sol–gel methods that incorporated transition metals (Ti or V) into the final dendrimer-templated mesoporous silicate structures (see figure 2). The synthesis procedure was adapted from the work by Larsen

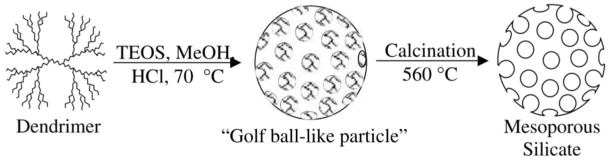

Figure 2. Pathway for the formation of the dendrimer-templated mesoporous materials.

Table 1
Molar ratios of reactants for DAB-Am dendrimer-templated materials

Reagents	sol–gel Molar Ratios[a]			
	CU-D32-Ti	CU-D32-V	CU-D64-Ti	CU-D64-V
Tetraethylorthosilicate	1.0	1.0	1.0	1.0
1-Propanol	4.241	4.241	4.241	4.241
Methanol	3.598	3.598	3.598	3.598
HCl	0.006068	0.006068	0.006068	0.006068
Water	2.806	2.806	2.806	2.806
CU-D32	0.02319	0.02319	0.0	0.0
CU-D64	0.0	0.0	0.01137	0.01137
Titanium isopropoxide (2 wt%)	0.01535	0.0	0.01535	0.0
Titanium isopropoxide (10 wt%)	0.08358	0.0	0.08358	0.0
Vanadium oxide (2 wt%)	0.0	0.008181	0.0	0.008181
Vanadium oxide (10 wt%)	0.0	0.04454	0.0	0.04454

[a]Only one molar ratio of active metal was selected for a given sample.

et al. [29–31] on dendrimer-templated siliceous materials, such as NU-1. The initial sol–gel was prepared by adding 1.03 g of tetraethyl orthosilicate (Aldrich, 98%) to a solution of 0.403 g of DAB-Am dendrimer (CU-D32 or CU-D64 DSM, Netherlands, 97%) in 1.26 g of 1-propanol (Fisher, 99.5%). Upon stirring, the solution turned cloudy due to the formation of a small amount of precipitate; however, it remained inviscid. To this homogeneous solution was added 0.57 g of methanol (Fisher, 99.9%), and the mixture was again vigorously stirred. For materials containing titanium or vanadium, the appropriate transition metal precursor was added with stirring. Titanium isopropoxide (Aldrich, 97%) was used as the titanium precursor, and vanadium oxide (Aldrich, 99.6%) was the precursor for vanadium-doped materials. Table 1 shows the molar ratios of reactants used for preparing the dendrimer-templated materials. The notation for sample naming is D-M-Y where D represents CU-DX (X = number of amine terminating groups on dendrimer, 32 or 64), M represents either Ti or V metal, and Y is the weight loading of metal oxide that would be present in the final silicate material if all the silicon and metal precursors in the initial sol–gel were precipitated as oxide product and does not necessarily reflect the amount of metal oxide content in the final product. The molar ratio of dendrimer template in the sol–gel was adjusted so that a constant number of amine terminating groups would be present (i.e., CU-D64 has twice as many amine terminating groups per molecule as CU-D32; thus, the molar ratio for the larger dendrimer is half that of the smaller).

The final sol–gel mixture was then transferred to a non-stirred teflon-lined steel autoclave equipped with a rupture disk (Parr) and heated in a convection oven at 100 °C for 15 min. The autoclave was then carefully removed from the oven and allowed to cool. Upon cooling, the cap was removed from the liner, and 0.25 g of 0.12 M hydrochloric acid was added. With the addition of HCl to the solution, rapid gelation occurred, and the solution viscosity increased significantly. The gel was again stirred vigorously, and the autoclave assembly was resealed and placed in a convection oven at 70 °C for 12 h.

After 12 h, the autoclave was removed from the oven and allowed to cool to room temperature. The contents of the teflon liner were placed into a polypropylene centrifuge tube along with deionized water. The aqueous mixture was vigorously stirred with a spatula to produce a homogeneous suspension. The mixture was centrifuged, and the resulting liquid was poured off the solid. This washing procedure was repeated three more times. Finally, the wet solid product was transferred to a ceramic dish and dried in a convection oven at 100 °C for approximately 12 h. Once dry, the sample was weighed and transferred to a sealed sample vial for storage.

The dendrimer template was removed from the silicate structure by first drying the sample for 24 h at 100 °C in a convection oven, then calcining the sample in a furnace under nitrogen flow at 560 °C for 3 h using the heating protocol developed by Larsen and co-workers [29–30]. Further calcination of the product was achieved by heating the sample under constant air flow at 560 °C for 2 h.

2.2. Characterization

Atomic absorption (AA) spectroscopy and combustion analyses (Galbraith Laboratories) were used for elemental analysis of the calcined metal-doped CU-D64 samples. The reported total metal content of the samples are shown in table 2.

Temperature-programed pyrolysis and oxidation analysis was performed on the uncalcined CU-D32-Ti-2 and CU-D64-Ti-2 samples. These experiments were performed using a TA instruments thermogravimetric analyzer (AutoTGA 2950, High Resolution, V5.4A). Milligram weight samples were analyzed in both air and

Table 2
Atomic absorption spectroscopy analysis of calcined metal-doped CU-D64 samples

Sample ID	Analysis	Weight percent (%)
CU-D64-Ti-2	Titanium	0.96 ± 0.1
CU-D64-Ti-10	Titanium	8.59 ± 0.1
CU-D64-V-2	Vanadium	1.80 ± 0.1
CU-D64-V-10	Vanadium	6.39 ± 0.1

nitrogen atmospheres to determine the effect of O_2 on degradation behavior. For each sample, the weight was recorded as the sample was heated at a rate of 10 °C min^{-1} from ambient temperature to 100 °C, held isothermally for 30 additional minutes, and then heated further at a rate of 10 °C min^{-1} to 600 °C.

SEM images of the samples were taken with a Hitachi S-3500N microscope in order to determine particle morphology and average particle size. Before analysis, the powdered samples were mounted on carbon stubs with the help of double adhesive tape. The samples were then coated with a thin layer of gold in a Hummer 6.2 sputtering unit to prevent sample charging during SEM analysis. Finally, SEM digital images were collected with the electron beam kept at 20 kV.

Energy dispersion X-ray analysis (EDX) was used to determine metal dispersion for selected samples. Specifically, it provided information about whether the catalytically active metal atoms (Ti or V) were incorporated randomly throughout the particles or if these metal atoms formed a separate oxide phase.

Powder X-ray diffraction (PXD) experiments were performed on selected calcined samples using a SCINTAG XDS-2000 diffractometer with CuK_α radiation. These data were used to ascertain product crystallinity and pore size distribution as well as the presence of any impurity phases. Small slits were used on both the source and detector so as to allow for the detection of low angle diffraction peaks. Only data within the 2-theta range of 2–10 are shown since there were no significant peaks observed at higher 2-theta angles.

In order to confirm that the modified synthesis procedure was successful in producing a mesoporous material with high surface area, each calcined sample was tested using a Micromeritics ASAP 2010 surface area analyzer equipped with Micromeritics Version 5.02 software. Prior to testing, each sample was degassed under vacuum at 150 °C for at least 6 h. Once degassed, a standard 5-point nitrogen BET surface area analysis was performed on each sample.

The ASAP 2010 was also used to determine the microporosity and mesoporosity of catalyst samples as a continuous distribution of pore volume with respect to pore size. Approximately 0.1 g of a calcined sample was first degassed for 12 h at 200 °C in a sample tube. Next, the free space of the sample and sample holder was measured using helium (UHP grade). Upon completion of free space measurements, the sample was again degassed for 12 h at 200 °C to remove all residual helium. Finally, pore volume analysis was performed using nitrogen (UHP grade). The Horvath and Kawazo [33] correction for spherical pore geometry was used with the interaction parameter calculated for nitrogen adsorbing onto aluminosilicate materials because there were no parameters available for pure silicate materials.

2.3. Reaction studies

The catalytic activity and selectivity of the dendrimer-templated catalysts was ascertained from kinetic studies that involved the oxidation of cyclohexene by tert-butyl hydroperoxide (TBHP). There were several possible oxidation products that could be formed (e.g., 1,2-dihydroxy cyclohexene); however, reaction studies showed that only cyclohexene oxide and tert-butanol were formed under mild reaction conditions (see figure 3).

The reactions were conducted in a slurry batch reactor equipped with a reflux condenser at approximately 60 °C for 7–8 h at atmospheric pressure. The reactor consisted of a glass reaction flask that was partially submerged in a temperature-controlled oil-bath. The reactor and oil bath were continuously stirred to ensure the system was well mixed and isothermal. Predetermined amounts of cyclohexene (Aldrich, 99%), acetonitrile (Fisher, 99.9%), and catalyst were weighed, added to the reactor, and allowed to warm to the desired reaction temperature. Finally, TBHP (Fisher, 5–6 M in Decane) was added to the reactor. All reagents were used as received without further purification.

Acetonitrile was used as a solvent in selected runs in order to conduct reaction studies at varying reagent concentrations. The initial concentrations of TBHP, cyclohexene, and acetonitrile were varied from 1.5 to 3.0, 4.0 to 6.5, and 0 to 6.5 molar, respectively. Approximately 0.30 g of catalyst was used in each reaction. Samples of the reaction mixture (40–120 μL) were taken at regular intervals (30 or 60 min) during the reaction. These samples were diluted with methanol and an internal standard and were immediately analyzed using a Hewlett Packard (HP) 6890 Gas Chromatograph equipped with an HP 5973 Mass Selective Detector. The resulting peaks were integrated using HP software (Chemstation 61707BA version B.01.00), and the species concentrations were calculated from previously developed calibration curves. The reproduc-

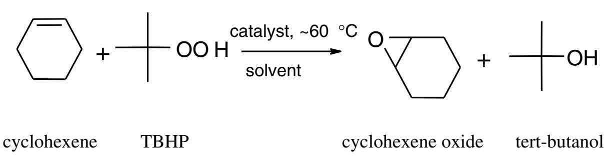

Figure 3. Catalytic oxidation of cyclohexene by TBHP.

ibility of species concentration by GCMS was approximately 4%, with the exception of the TBHP concentration, which varied as much as 40% due to thermal degradation during analysis.

The variation in species concentration with time during a given reaction study allowed for the calculation of pseudo rate constants and species conversions. These reaction data were then used to ascertain reaction order parameters for a power law rate model of the oxidation reaction. No attempts were made to quantify temperature dependent parameters (i.e., a single temperature rate constant rather than an Arrhenius law model was used).

3. Results and discussion

3.1. Elemental analysis

The AA spectroscopy analysis showed that the titanium and vanadium loadings were slightly less than would be expected from the synthesis gel stoichiometry (see table 2); however, this trend in metal loading is common for doped silicate materials prepared by sol–gel techniques [19,34]. Carbon analysis results (not shown) for representative calcined samples indicated that only trace levels of carbon were present, which indicates that the bulk of the dendrimer template and organic solvents were removed by calcination.

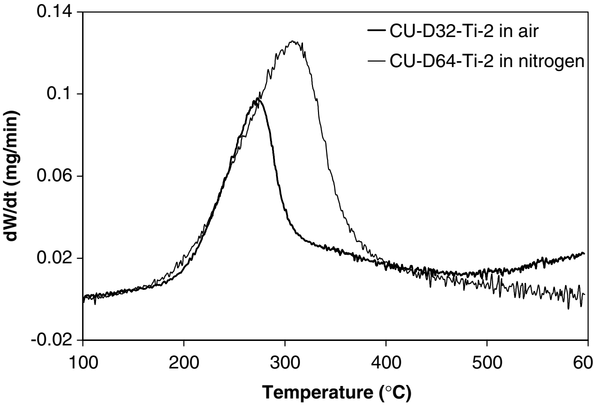

Figure 4. Temperature-programed oxidation of CU-D32-Ti-2 and temperature-programed pyrolysis of CU-D64-Ti-2.

3.2. Temperature-programed pyrolysis and oxidation analysis

The temperature-programmed pyrolysis and oxidation (TPP and TPO) behavior of titanium-doped materials, CU-D32-Ti-2 in air and CU-D64-Ti-2 in nitrogen, are shown in figure 4. These results show that the encapsulated dendrimer templates begin to decompose at about 150 °C and are fully decomposed at 500 °C. Comparing the results from TPP and TPO experiments showed that oxygen enhanced the rate of dendrimer decomposition at temperatures above 200 °C, but the temperature required for final dendrimer removal was similar for the two experiments. Further comparison of these results to those reported by Larsen *et al.* [29] for similar non-doped dendrimer-templated silicates reveals that the temperature needed to initiate dendrimer decomposition in titanium-doped samples is approximately 108 °C lower than that required for decomposition in transition metal free silicates. From this data, one can infer that the titanium dopant is near the surface of the silicate and catalyzes the decomposition of the template at elevated temperatures. These results also confirm that the dendrimers are stable at the synthesis temperature of 70 °C and are burned out at the calcination temperature of 560 °C. Observed sample weight loss at temperatures above 560 °C can be attributed to the escape of trapped gases from the interior of the materials as well as the condensation of neighboring silanols on the silicate surface to yield oxides and water vapor.

3.3. SEM and EDX

SEM analysis indicates that the average particle sizes of the CU-D32 and CU-D64 samples were approximately 0.15 and 0.20 μm, respectively. From the EDX analysis, it was seen that in both titanium and vanadium-doped samples, the metal atoms were randomly dispersed throughout the solid structure. See figure 5 for representative SEM and EDX of calcined CU-D64-Ti-2.

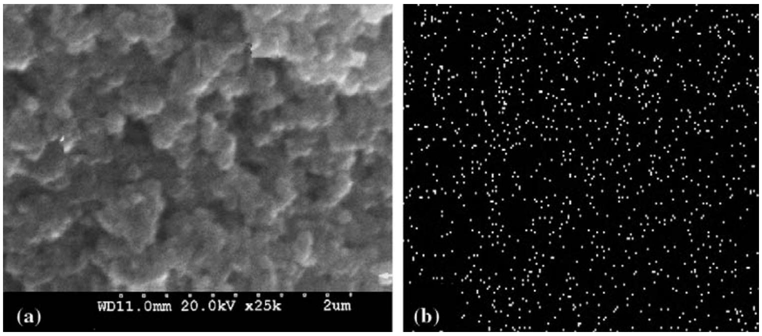

Figure 5. (a) Representative SEM of calcined CU-D64-Ti-2 and (b) EDX of calcined CU- D64-Ti-2 showing the titanium metal well dispersed in the sample.

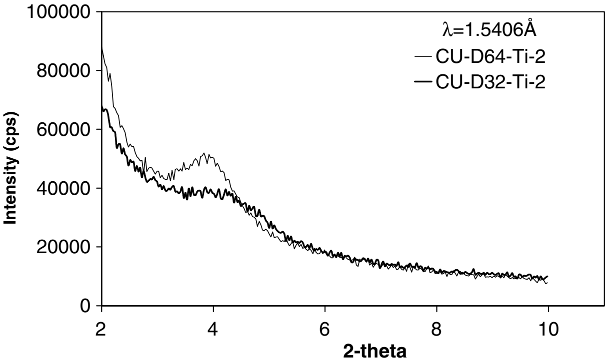

Figure 6. Powder X-ray diffraction results for CU-D32-Ti-2 and CU-D64-Ti-2.

3.4. PXD analysis

Representative PXD patterns are shown in figure 6 for both CU-D32-Ti-2 and CU-D64-Ti-2. Broad peaks at 2-theta values of 4.1 and 3.83 were obtained for the CU-D32-Ti-2 and CU-D64-Ti-2, respectively. These 2-thetavalues corresponded to a d-spacing of 21.5 and 23 Å, respectively. While the distance calculated from the spectra is not an exact measure of the pore size, it does indicate the repeating distance of structural features within the sample. Since the spacing between structural features increases with increasing dendrimer generation, this data demonstrates that the pore size of the final catalyst material is directly dependant upon the size of the dendrimer used to create it. Additionally, PXD data showed that the dendrimer templated materials exhibited less crystallinity than is often observed with hexagonally packed mesoporous materials (e.g., MCM-41).

3.5. BET surface area

The average surface areas calculated by 5-point nitrogen BET analysis are shown in table 3 for selected uncalcined and calcined forms of dendrimer-templated samples and MCM-41 materials. The MCM-41 materials are listed primarily for comparison purposes. Surface areas for the calcined dendrimer-templated materials ranged from 500 to 700 $m^2\ g^{-1}$, while the MCM-41 materials had noticeably higher surface areas. In general, the metal-doped dendrimer-templated materials had lower surface areas than comparable samples that were pure silicates; however, the exact cause for this decrease in surface area was not investigated. Post-reaction surface area analysis of selected samples indicated that both the titanium and vanadium-doped materials had a decrease in surface area that ranged from approximately 80 to 150 $m^2\ g^{-1}$.

Table 3
Average Nitrogen BET surface area results for selected uncalcined and calcined mesoporous materials

Sample	Number of samples	Average BET surface area ($m^2\ g^{-1}$)
Uncalcined samples		
CU-D32	1	8.5 ± 0.1[a]
CU-D64	1	17.4 ± 0.1[a]
Calcined samples		
CU-D32	1	684 ± 19[a]
CU-D64	1	661 ± 13[a]
CU-D32-Ti-2	6	575 ± 41[b]
CU-D32-Ti-10	2	500 ± 54[b]
CU-D64-Ti-2	4	575 ± 39[b]
CU-D64-Ti-10	3	635 ± 52[b]
CU-D32-V-2	2	588 ± 35[b]
CU-D32-V-10	5	535 ± 67[b]
CU-D64-V-2	3	636 ± 79[b]
CU-D64-V-10	3	501 ± 75[b]
MCM-41-Ti-2	2	1054 ± 56[b]
MCM-41-V-2	1	846 ± 32[a]

[a] instrumentation error for a single analysis.
[b] standard deviation for multiple analyses.

3.6. Micropore volume analysis

Pore volume analysis was used to gain additional insight into the size and geometry of pores generated by the dendrimer templates. Representative differential pore volume distribution plots are shown in figure 7 for CU-D32-Ti-2 and CU-D64-Ti-2 samples. This plot shows that the dominant pore size for the CU-D32-Ti-2 and the CU-D64-Ti-2 materials is 11.8 and 13.1 Å, respectively. Thus, the difference in pore sizes for materials templated by either 4th or 5th generation dendrimers is approximately 1.3 Å. This compares well to the 1.5 Å d-spacing difference observed with the PXD data of comparable samples.

3.7. Reaction studies

The catalytic activity of all materials was tested using cyclohexene epoxidation as the test reaction. Analysis of cyclohexene oxidation products shows that all catalyst materials tested are very selective in the production of cyclohexeneoxide under mild oxidative conditions. In only a few selected runs were detectable quantities of

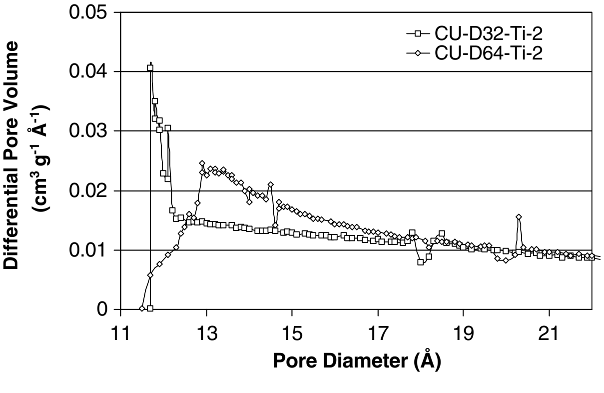

Figure 7. Pore volume distribution for CU-D32-Ti-2 and CU-D64-Ti-2.

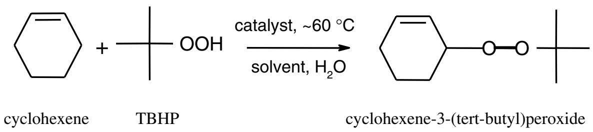

Figure 8. Catalytic oxidation of cyclohexene by TBHP in the presence of water.

any side products involving cyclohexene derivatives observed. In those runs, water was added to the reactor to examine its effect on catalyst deactivation. Those reactions to which water was added produced no cyclohexeneoxide; however, they did produce significant amounts of cyclohexene-3-(t-butyl)peroxide (see figure 8). In reactions where pure silicate mesoporous materials were used, no conversion of cyclohexene was observed. Finally, a limited number of experiments using the same catalyst, temperature, and reactant concentration were conducted at varying stirring speeds. As there was no observable variation in reaction rate with stirring rate, bulk diffusion phenomena did not appear to be limiting the rate of reaction.

Representative kinetic data for the epoxidation of cyclohexene using several mesoporous catalysts are given in table 4. The data show that the titanium-doped, CU-D64-templated materials have slightly higher average rates of reaction as compared to titanium-doped MCM-41 materials, while having comparable reaction orders. It is also noteworthy to mention that the CU-D64-templated materials perform measurably better than the CU-D32 materials as one might expect due to larger pore sizes and therefore, more accessible surface area. It was observed that the reaction rates did not vary significantly with catalyst metal loading. This is likely due to their being comparable levels of active metal species at the surfaces of the CU-DXX-M-2 and CU-DXX-M-10 catalysts; however, this was not experimentally verified. This latter assumption is supported by the idea that there should be a limit to the amount of active metal species that can be located near or at the catalyst surface, and any increase in metal loading above this limit would simply increase the concentration of that species in the bulk phase of the catalyst, where it is unavailable for catalysis.

The average turnover frequency (TOF) and turnover number (TON) for vanadium and titanium-doped catalysts based on total metal loading and cyclohexene conversion percent are shown in table 4. Most of these values are comparable to those found previously for cyclohexene epoxidation reactions using similarly prepared metal-doped MCM-41 materials [18–20]. For example, Oldroyd *et al.* [20]observed a TOF to cyclohexene oxide of 33.8 h^{-1} for a Ti-MCM-41 catalyst containing 1.73 wt% Ti. However, the average TOF for the CU-D64-Ti-2 is approximately a factor of 2 greater than the TOF commonly observed for the epoxidation of cyclohexene by MCM-41 materials containing equivalent titanium loadings [19–20]. It is unlikely that the electronic configuration of the active metal site in titanium-doped MCM-41 materials differs significantly from that present in CU-D64-Ti-2; thus, the increase in TOF must result from the CU-D64-Ti-2 catalyst having either an increased ratio of surface to bulk titanium species or a more favorable extended catalyst structure that stabilizes the reaction intermediate or enhances the rate of reactant adsorption or product desorption. It was also observed that the TOF decreased over time, which is to be expected in a batch reactor system where the concentration of reactant is decreasing with time.

4. Conclusions

This work has demonstrated that dendrimer-templated mesoporous oxidation catalysts can easily

Table 4
Average kinetic data for the catalyzed epoxidation of cyclohexene using TBHP

Sample	Runs	$k \times 10^3 (\mathrm{mol} \cdot \mathrm{l}^{-1})^{1-\alpha-\beta}$/g cat	$k^* (\mathrm{mol} \cdot \mathrm{l}^{-1})^{1-\alpha-\beta}$/g metal	α	β	TOF[a] h^{-1}	TON[b]
CU-D32	1	0.0	–	–	–	–	–
CU-D64	3	0.0	–	–	–	–	–
CU-D32-Ti-2	6	5.20 ± 1.3	–	0.91 ± 0.11	0.03 ± 0.05	–	–
CU-D64-Ti-2	3	9.31 ± 1.7	0.970 ± 0.18	0.92 ± 0.10	0.02 ± 0.01	98.0	513
CU-D32-Ti-10	2	4.34 ± 2.4	–	0.90 ± 0.05	0.00 ± 0.01	–	–
CU-D64-Ti-10	5	9.43 ± 1.7	0.110 ± 0.02	0.90 ± 0.13	0.15 ± 0.17	17.3	57
CU-D32-V-2	3	2.50 ± 0.8	–	0.98 ± 0.03	0.00 ± 0.01	–	–
CU-D64-V-2	2	5.71 ± 2.4	0.317 ± 0.13	0.94 ± 0.08	0.00 ± 0.01	56.8	196
CU-D32-V-10	4	3.72 ± 0.5	–	0.92 ± 0.06	0.01 ± 0.01	–	–
CU-D64-V-10	4	6.48 ± 3.7	0.101 ± 0.06	0.86 ± 0.09	0.00 ± 0.01	14.2	54
MCM-41-Ti-2	2	5.80 ± 2.0	–	0.93 ± 0.05	0.02 ± 0.03	–	–
MCM-41-V-2	4	7.16 ± 3.6	–	0.85 ± 0.21	0.03 ± 0.05	–	–

[a] TOF = average turn over frequency based on metal loading and cyclohexene conversion.
[b] TON = average turn over number based on total metal loading.

be produced to have similar physical and chemical properties to MCM-41 materials. In addition, it has also been shown that the pore sizes of the resulting mesoporous materials can be tuned by using dendrimers of different sizes as the templating agent in creating these materials. These materials readily incorporate small amounts of either titanium or vanadium into the silicon matrix with only a relatively small loss of surface area in the resulting catalyst material. Even with the significant difference in surface area, the dendrimer-templated materials containing catalytically active transition metals have reaction rates and reaction orders comparable to micelle-templated materials having similar metal loading for the epoxidation of cyclic alkenes.

Acknowledgment

The authors acknowledge the assistance of David Kuhnell, Alex Rhue, and Christopher McDonald with conducting BET surface area measurements and partial oxidation reaction studies. The authors also acknowledge the financial support of the National Science Foundation (CAREER 9985022) and the South Carolina Commission on Higher Education (R99-06C).

References

[1] I.W.C.E. Arends and R.A. Sheldon, Appl. Catal. A Gen. 212 (2001) 175.

[2] R.A. Sheldon and J. Dakka, Catal. Today 19 (1994) 215.

[3] R.A. Sheldon and J.K. Kochi, *Metal Catalyzed Oxidations of Organic Compounds*, (Academic Press, New York, 1981).

[4] R.A. Sheldon, Chemtech (1991) 566.

[5] G. Centi and M. Misono, Catal. Today 41 (1998) 287.

[6] J.S. Rafelt and J.H. Clark, Catal. Today 57 (2000) 33.

[7] M.G. Clerici, Topics Catal. 13 (2000) 373.

[8] N.N. Trukhan, V.N. Romannikov, A.N. Shmakov, M.P. Vanina, E.A. Paukshtis, V.I. Bukhtiyarov, V.V. Kriventsov, I.Yu. Danilov and O.A. Kholdeeva, Micropor. Mesopor. Mat. 59 (2003) 73.

[9] A. Tuel and L.G. Hubert-Pfalzgraf, J. Catal. 217 (2003) 343.

[10] P.T. Tanev, M. Chibwe and T. Pinnavaia, Nature 368 (1994) 321.

[11] L.Y. Chen, G.K. Chuah and S. Jaenicke, Catal. Lett. 50 (1998) 107.

[12] A. Corma, Chem. Rev. 97 (1997) 2373.

[13] A. Sayari, Chem. Mater. 8 (1996) 1840.

[14] J.S. Beck, J.C. Vartuli, W.J. Roth, M.E. Seonowicz, C.T. Kresge, K.D. Schmitt, C.T-W. Chu, D.H. Olson, E.W. Sheppard, S.B. McCullen, J.B. Higgins and J.L. Schlenker, J. Am. Chem. Soc. 114 (1992) 10834.

[15] W. Zhang, M. Froba, J. Wang, P.T. Tanev, J. Wong and T.J. Pinnavaia, J. Am. Chem. Soc. 118 (1996) 9164.

[16] K.A. Koyano and T. Tatsumi, Micropor. Mater. 10 (1997) 259.

[17] A. Vinu, J. Dedecek, V. Murugesan and M. Hartmann, Chem. Mater. 14 (2002) 2433.

[18] L.X. Dai, K. Tabata, E. Suzuki and T. Tatsumi, Chem. Mater. 13 (2001) 208.

[19] L.Y. Chen, G.K. Chuah and S. Jaenicke, Catal. Lett. 50 (1998) 107.

[20] R.D. Oldroyd, G. Sankar, J.M. Thomas and D. Özkaya, J. Phys. Chem. B 102 (1998) 1849.

[21] C. Howard, *The Synthesis and Catalytic Properties of Novel Heterogeneous Oxidation Catalysts. PhD Dissertation* (Clemson University, Clemson, SC, 2000).

[22] T. Blasco, A. Corma, M.T. Navarro and J.P. Pariente, J. Catal. 156 (1995) 65.

[23] G. Tasi, I. Pálinkó, Á. Molnár and I. Hannus, J. Mol. Struct. (THEOCHEM) 666–667 (2003) 69.

[24] P.B. Weisz, Pure Appl. Chem. 52 (1980) 2091.

[25] P.B. Weisz, ACS Symp. Ser. 738 (1999) 18.

[26] S.M. Csicsery, Pure Appl. Chem. 58 (1986) 841.

[27] S.M. Csicsery, Stud. Surf. Sci. Catal. 94 (1995) 1.

[28] G. Larsen, E. Lotero and M. Marquez, J. Phys. Chem. B. 104 (2000) 4840.

[29] G. Larsen, E. Lotero and M. Marquez, J. Mater. Res. 15 (2000) 1842.

[30] G. Larsen, E. Lotero and M. Marquez, Chem. Mater. 12 (2000) 1513.

[31] G. Larsen and R. Velarde-Ortiz, Chem. Mater. 14 (2002) 858.

[32] A. Gong, Y. Chen, X. Zhang, H. Liu, C. Chen and F. Xi, J. Appl. Polym. Sci. 78 (2000) 2186.

[33] G. Horvath and K. Kawazoe, J. Chem. Eng. Jpn. 16 (1983) 470.

[34] P. Wu and T. Tatsumi, Chem. Mater. 14 (2002) 1657.